Research article

Long noncoding RNA SNHG6 promotes the malignant phenotypes of ovarian cancer cells via miR-543/YAP1 pathway

Mengya Su [a],[*], Ping Huang [b], Qian Li [b]

[a] *Department of Reproductive Medicine, Cangzhou Central Hospital, Cangzhou, 061000, Hebei Province, China*
[b] *Department of Gynecology, Cangzhou Central Hospital, Cangzhou, 061000, Hebei Province, China*

A R T I C L E   I N F O

A B S T R A C T

The long non-coding RNA small nucleolar RNA host gene 6 (SNHG6) acts as an oncogene in several cancers, and is highly expressed in ovarian cancer. MiR-543, a tumor suppressor, was expressed lowly in ovarian cancer. However, whether SNHG6 performed its oncogenic role via miR-543 in ovarian cancer, as well as the underlying mechanism is still not clear. In this study, we showed that the levels of SNHG6 and Yes-associated protein 1 (YAP1) were significantly elevated, while the level of miR-543 was significantly decreased, in ovarian cancer tissues compared with adjacent normal samples. We demonstrated that overexpression of SNHG6 significantly promoted the proliferation, migration, invasion and epithelial-mesenchymal transition (EMT) of ovarian cancer cells SKOV3 and A2780. Knockdown of SNHG6 showed the opposite effects. MiR-543 level was negatively correlated with the SNHG6 level in ovarian cancer tissues. SHNG6 overexpression significantly inhibited the expression of miR-543, and SHNG6 knockdown significantly elevated the expression of miR-543 in ovarian cancer cells. The effects of SNHG6 on ovarian cancer cells were abrogated by miR-543 mimic, and strengthened by *anti*-miR-543. YAP1 was identified as a target of miR-543. Forced expression of miR-543 significantly inhibited the expression of YAP1. Moreover, YAP1 overexpression could reverse the effects of SNHG6 downregulation on the malignant phenotypes of ovarian cancer cells. In summary, our study showed that SNHG6 promoted the malignant phenotypes of ovarian cancer cells via miR-543/YAP1 pathway.

1. Introduction

Ovarian cancer is the most deadly gynaecological cancer [1]. It accounts for 2.5% of all malignancies among females, with a mortality rate ranging up to 5% [2]. The high mortality is mainly due to the advanced stage of diagnosis [2]. Although many patients can achieve an initial disease-free interval, most of the patients will eventually relapse [3]. Therefore, it is important to explore the molecular mechanism of ovarian cancer progression to improve the prognosis of patients.

Accumulating evidences revealed that long non-coding RNAs (lncRNAs) are aberrantly expressed and involved in the progression of ovarian cancer. The lncRNA small nucleolar RNA host gene 6 (SNHG6) is located in chromosome 8q13.1 [4]. Studies showed that the SNHG6 level was elevated and functioned as an oncogene in multiple cancers, such as liver cancer [4], gastric cancer [5], colorectal cancer [6], bladder cancer [7], and breast cancer [8]. A meta-analysis revealed that SNHG6 expression was significantly upregulated and was correlated with poor overall survival in a variety of tumors [9]. Recently, it was showed that the SNHG6 promoted the

---

* Corresponding author.
E-mail address: sma4323820@163.com (M. Su).

proliferation, migration and invasion of ovarian cancer cells, as well as tumor growth in nude mice [10].

LncRNAs mainly act as a competing endogenous RNA (ceRNA) to modulate distribution of microRNAs on their target genes, leading to an additional level of post-transcriptional regulation [11]. In breast cancer and glioma, SNHG6 was reported to promote tumor progression by acting as a miR-543 sponge [12,13]. MiR-543 was reported to serve as a tumor suppressor in ovarian cancer, and the expression of miR-543 was significantly decreased in ovarian cancer cell lines and ovarian cancer tissues [14]. Upregulation of miR-543 led to increased cell supernatant glucose levels and suppressed cell growth via targeting insulin-like growth factor 2 (IGF2) [14]. MiR-543 could also suppress the proliferation and invasion in ovarian cancers by targeting TWIST1 [15]. However, whether SNHG6 performed its oncogenic role via miR-543 in ovarian cancer, as well as the underlying mechanism is still not clear. In this study, we aimed to verify the function of SNHG6 in ovarian cancer, and to explore the underlying mechanism.

2. Materials and methods

2.1. Human tissues collection

Thirty-two primary epithelial ovarian cancer tissues and adjacent normal ovarian epithelial specimens were collected from patients who underwent surgery at the Cangzhou Central Hospital from January 2017 to April 2019. Inclusion criteria: patients met the diagnostic criteria for ovarian cancer; patients would undergo surgical treatment; no local or systemic treatment prior to the operation. Exclusion criteria: patients with infectious diseases, injury of important organs or malignant tumors; patients with diseases of heart, kidney, liver and other vital organs; patients with mental or mental illness. Informed consents had been signed by all patients prior to enrolling in the study. The collected tissues were separately confirmed by two pathologists in a blinded manner. Then, samples were kept in liquid nitrogen immediately until use for quantitative real-time PCR (qRT-PCR). The clinical characteristics of patients were shown in Table 1. This study was followed with all criteria adhered to the Declaration of Helsinki, and had been approved by the ethics committee of the Cangzhou Central Hospital (approval number: CCH-2017-Y-023).

2.2. Power calculation

Since it is difficult to estimate the level of SNGH6 in ovarian cancer based on the literatures, the required sample size was hard to be estimated. The post-hoc power analysis was performed using GPower software (version: 3.1.9.2). The value of α err prob was set as 0.05. The t-test and two-tail were selected.

2.3. Cell culture and transfection

Human ovarian cancer cell lines (SKOV3 and A2780) and normal ovarian cell (IOSE80) were used in this study. The cell authentication was confirmed by short tandem repeat (STR) characterization. SKOV3 cells were purchased from the Cell Bank of the Chinese Academy of Sciences (Shanghai, China). A2780 and IOSE80 cell lines were purchased from ATCC (VA, USA). RPMI-1640 medium supplemented with 10% fetal bovine serum (FBS; Gibco, Waltham, MA, USA) was used for cell culture. These cells were maintained in a humidified incubator set at 37 °C with 5% CO_2. MiR-543 mimic/*anti*-miR-543 were designed and synthesized by GenePharma (Shanghai, China). The pcDNA3.1-SNHG6, pLVX-SNHG6-shRNA and pcDNA3.1-YAP1 plasmids were constructed by

Table 1
The clinicopathological characteristics and expression of SNHG6, miR-543 and YAP1 in ovarian cancer patients ($n = 32$).

Characteristics	Number	SNHG6			miR-543			YAP1		
		Low (n)	High (n)	P	Low (n)	High (n)	P	Low (n)	High (n)	P
Age				0.479			0.035*			0.314
<50	15	8	7		5	10		8	7	
≥50	17	10	7		12	5		12	5	
Histological subtype				0.645			0.19			0.626
Serous	27	13	14		13	14		13	14	
Other	5	2	3		4	1		3	2	
Ascites				0.433			0.694			0.006*
Yes	23	10	13		11	12		8	15	
No	9	6	3		5	4		8	1	
Grade				0.036*			0.012*			0.072
G1/G2	13	9	4		3	10		9	4	
G3	19	6	13		13	6		7	12	
FIGO stage				0.022*			0.127			0.022*
I/II	10	8	2		3	7		8	2	
III/IV	22	8	14		13	9		8	14	
Lymph node metastasis				0.008*			0.028*			0.004*
Negative	20	13	7		7	13		14	6	
Positive	12	2	10		9	3		2	10	

*$P < 0.05$.

Tolo Biotech (Shanghai, China). These vectors were used to modulate miR-543, SNHG6, and Yes-associated protein 1 (YAP1) expression, respectively. SKOV3 and A2780 cells were planted into appropriate cell plates and then transfected with the above vectors using Lipofectamine 3000 (Invitrogen, Carlsbad, CA, USA) according to the manufacturer's protocols.

2.4. MTT assay

SKOV3 and A2780 cells were seeded into 96-well plates and transfected with indicated SNHG6, miR-543, and YAP1 vectors for 24, 48, 72 and 96 h. Cell viability was examined by MTT assay kit (Solarbio, Beijing, China). After incubation for designed times, the medium was changed to fresh RPMI-1640 medium containing 5 mg/ml MTT, and then cells were maintained at 37 °C for 4 h 110 μl dissolved reagent was added to each well to dissolve the precipitate after the culture medium was discarded. The absorbance value of each well at 490 nm was detected by a microtiter plate reader (Bio-Tek, Winooski, VT, USA).

2.5. Migration and invasion assay

Cell migration was carried out using 24-well transwell chambers (8.0 μm pore size inserts). Cells were transfected with indicated vectors for 48 h, and then cell suspension was collected. Subsequently, 5×10^4 cells in serum-free medium were planted into the upper chamber. RPMI-1640 medium containing 20% FBS was added into the lower chamber. After 24 h of incubation at 37 °C, cells remaining on the upper side of the chambers were wiped off. The cells that migrated through the membrane were fixed with 4% formaldehyde, and were then stained with crystal violet solution (Solarbio, China) for 30 min. To detect the cell invasion, all the procedures were performed according to the migration assay except for the bottom of transwell chamber coated with BD Matrigel (BD Biosciences, San Diego, CA, USA). Cells in five randomly selected fields were counted under a light microscope.

2.6. Dual-fluorescence reporter gene analysis

Starbase V3.0 online tool revealed that SNHG6 contained the potential binding site of miR-543, and miR-543 might target Yes-associated protein 1 (YAP1). Hence, we constructed the SNHG6 and YAP1 wild-type (WT) or mutant-type (MUT) reporter vectors. In brief, fragments of SNHG6 and YAP1 with the predicted miR-543 binding sites were amplified and inserted into pmirGLO luciferase reporter vector (Promega, Madison, WI, USA). Also, the mutant sequences of miR-543 binding sequences were also inserted into the luciferase reporter vector. The constructed plasmids and miR-543 mimic or its control mimic were co-transfected into SKOV3 and A2780 cells with Lipofectamine 3000 (Invitrogen). After 48 h, cells were lysed to detect relative luciferase activity using dual-luciferase reporter assay system (Promega, Madison, WI, USA) according to the manufacturer's instructions.

2.7. Quantitative real-time PCR

Total RNA was isolated from human tissues and cells using TRIzol reagent (Invitrogen). RNA was reverse-transcribed into cDNA for mRNA and miRNA using HiFiScript gDNA Removal cDNA Synthesis Kit and miRNA cDNA Synthesis Kit (both were from CWBIO, Beijing, China). The RNA levels of SNHG6, E-cadherin, N-cadherin, vimentin and YAP1 were analyzed by TransStart Tip Green qPCR SuperMix (Transgen biotech, Beijing, China). The expression of miR-543 was determined using miRNA qPCR Assay Kit (CWBIO). The relative mRNA levels of target genes and miR-543 were calculated according to the $2^{-\Delta\Delta Ct}$ method. GAPDH or small nuclear RNA U6 was introduced as internal control. All primers were purchased from Sangon Biotech (Shanghai, China). And the sequences are as follows: SNHG6 forward 5′-AGCCTTTGAGGTGAAGGTGT-3′, reverse 5′-ATGCTCAATACATGCCGCGT-3'; YAP1 forward 5′-CCCTCGTTTTGCCATGAACC-3′, reverse 5′-GTTGCTGCTGGTTGGAGTTG-3'; E-cadherin forward 5′-TGAAAACAGCAAAGGGCTTGGA-3′, reverse 5′-GCAGTGTCTCTCCAAATCCGA-3'; N-cadherin forward 5′-ATGCCCGGTTTCATTTAGGGG-3′, reverse 5′-GGCATTGG-GATCGTCAGCAT-3'; vimentin forward 5′-CGGGAGAAATTGCAGGAGGA-3′, reverse 5′-AAGGTCAAGACGTGCCAGAG-3'; GAPDH forward 5′-TCGGAGTCAACGGATTTGGT-3′, reverse 5′-TTCCCGTTCTCAGCCTTGAC-3'; miR-543 forward 5′-ACACTCCAGCTGG-GAAACATTCGCGGTGC-3′, reverse 5′-CTCAACTGGTGTCGTGGA-3'; U6 forward 5′-CTCGCTTCGGCAGCACA-3′, reverse 5′-AACGCTTCACGAATTTGCGT-3'.

2.8. RNA immunoprecipitation

For RNA immunoprecipitation (RIP) assay, SKOV3 cells were lysed in RIP lysis buffer. The EZ-Magna RIP Kit (Millipore, Billerica, MA, USA) was used according to the manufacturer's instruction. Magnetic beads were conjugated with anti-AGO2 antibody (Millipore) or negative control IgG. The precipitated RNAs were subjected to quantitative real-time PCR (qRT-PCR) to measure the RNA levels of SNHG6, miR-543 and YAP1.

2.9. Western blot

Total proteins of SKOV3 and A2780 cells were lysed by RIPA Lysis Buffer (Beyotime, Beijing, China) containing PMSF. The protein concentration of each sample was analyzed by a BCA assay kit (Beyotime). Equal amounts of samples were loaded on 10% SDS-PAGE to separate proteins, and then transferred to a nitrocellulose membrane for the immunoblot process as described previously [16]. Primary antibodies were used at the following concentrations: *anti*-N-cadherin (1:1000; Cell Signaling Technology, Danvers, MA, USA),

anti-vimentin (1:1000; Abcam, Cambridge, MA, USA), anti-E-cadherin (1:1000; Abcam), and anti-YAP1 (1:500; Abcam). Protein bands were visualized with a BeyoECL Plus kit (Beyotime) and quantified using the ImageJ software (NIH, Bethesda, MD, USA) with normalization to GAPDH.

2.10. Statistical analysis

The data were expressed as mean ± standard deviation. GraphPad Prism 7.0 software (GraphPad Software, San Diego, CA, USA) was used for statistical analysis. Chi-square test was used to assay the correlation of SNHG6 expression and clinicopathological characteristics of ovarian cancer patients. The correlation between SNHG6 and miR-543 expression in ovarian cancer tissues was detected using Pearson's correlation analysis. Student's t-test was employed to analyze differences between two groups. One-way ANOVA followed by Bonferroni's multiple comparisons test was used to analyze differences for three or more groups. $P < 0.05$ was regarded to be statistically significant.

3. Results

3.1. SNHG6 levels were increased in ovarian cancer tissues and cells

The qRT-PCR data showed that SNHG6 levels were elevated in ovarian cancer tissues compared with the adjacent normal ovarian epithelial samples (2.59 [1.500, 3.263] vs 1.04 [0.898, 1.38], $P < 0.001$, Fig. 1A). Based on the levels of SNGH6 in ovarian cancer tissues and the adjacent normal ovarian epithelial samples, the effect size d was 1.2765. The calculated test power was 0.999. This indicated that the sample size of this study was sufficient and the results were credible.

Based on the median value of SNHG6 level in human ovarian cancer tissues, 16 patients were defined as high levels of SNHG6, and 16 patients were with low levels of SNHG6. The relationship between SNHG6 expression and patients' clinicopathological features were further analyzed. The levels SNHG6 were positively correlated with Grade, FIGO stage and lymph node metastasis of ovarian cancer patients (Table 1). Additionally, we also determined SNHG6 expression in ovarian cancer cell lines. As compared to normal ovarian IOSE80 cells, SNHG6 levels were increased in SKOV3 and A2780 ovarian cancer cells (Fig. 1B).

3.2. SNHG6 promotes proliferation, migration and invasion of ovarian cancer cells

Function of SNHG6 in ovarian cancer was investigated by modulating SNHG6 expression. Compared with the control group, pcDNA3.1-SNHG6 significantly upregulated SNHG6 expression, and SNHG6 shRNA downregulated SNHG6 expression (Fig. 2A). MTT assay showed that upregulation of SNHG6 remarkably promoted, while SNHG6 downregulation inhibited, the viability of SKOV3 and A2780 cells (Fig. 2B and C). Furthermore, the migration and invasion of SKOV3 and A2780 cells were elevated by transfection with pcDNA3.1-SNHG6, but reduced by transfection with pLVX-SNHG6-shRNA, as compared to the control group (Fig. 2D and E). These data indicate SNHG6 promotes the proliferation, migration and invasion of ovarian cancer cells.

3.3. SNHG6 facilitates the epithelial-mesenchymal transition of ovarian cancer cells

SNHG6 overexpression significantly elevated the mRNA levels of N-cadherin and vimentin, but reduced the mRNA levels E-cadherin in both SKOV3 and A2780 cells (Fig. 3A). Downregulation of SNHG6 notably decreased the mRNA levels of N-cadherin and
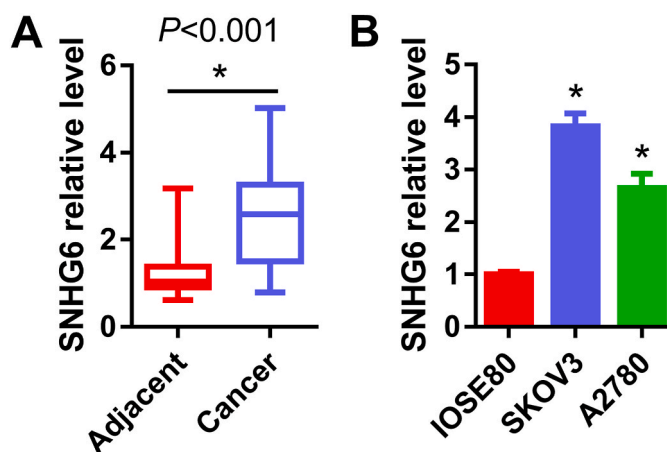

Fig. 1. SNHG6 expression is increased in ovarian cancer tissues and cells. (A) SNHG6 expression in 32 primary epithelial ovarian cancer tissues and adjacent normal ovarian epithelial samples was analyzed by real-time PCR. (B) SNHG6 expression was higher in human ovarian cancer cell lines (SKOV3 and A2780) than that in normal ovarian IOSE80 cells. *$P < 0.05$ vs the normal group or the IOSE80 cells.
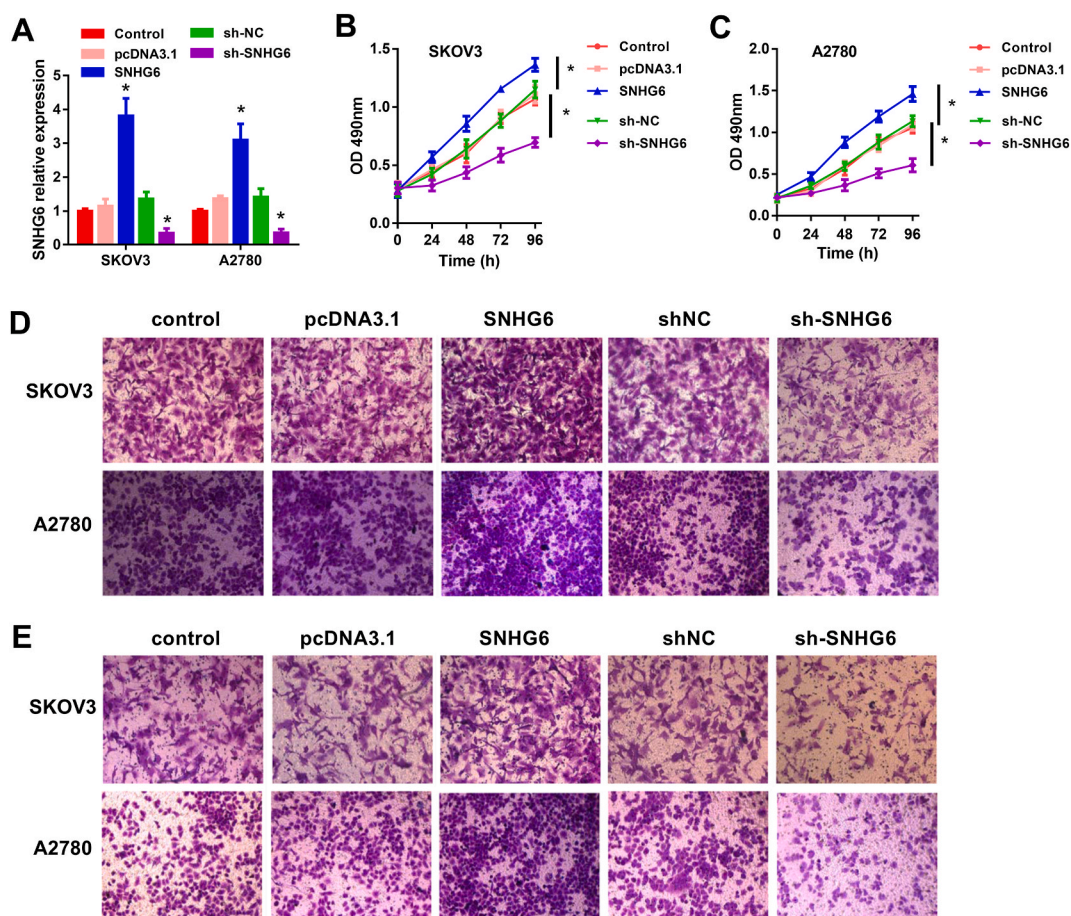
Fig. 2. SNHG6 promotes proliferation, migration and invasion of ovarian cancer cells. (A) SKOV3 and A2780 cells were transfected with empty pcDNA3.1 vector (pcDNA3.1), pcDNA3.1-SNHG6 (SNHG6), SNHG6 shRNA (sh-SNHG6) or their negative controls (sh-NC) for 48 h. SNHG6 expression was analyzed by qRT-PCR. SKOV3 (B) and A2780 (C) cells were transfected with designated vectors for 24, 48, 72, and 96 h, cell viability was detected by MTT. The migration (D) and invasion (E) of SKOV3 and A2780 cells were both determined by transwell. *$P < 0.05$ vs the control group.

vimentin, but up-regulated the mRNA levels of E-cadherin (Fig. 3A). The protein levels of N-cadherin, vimentin and E-cadherin were also confirmed by Western blot (Fig. 3B; The original images of blots in Fig. 3B were attached in supplementary file 1). These data indicate SNHG6 facilitates the epithelial-mesenchymal transition (EMT) of ovarian cancer cells.

3.4. SNHG6 functions through binding to and regulating miR-543 in ovarian cancer cells

Starbase online tool showed that SNHG6 possess a target site of miR-543 (Fig. 4A). The dual-fluorescence reporter gene assay demonstrated that miR-543 mimic remarkably inhibited the luciferase activity both in SKOV3 and A2780 cells transfected with wild-type SNHG6, but did not affect these cells transfected with the mutant vector, as compared to the control mimic (Fig. 4B). Upregulation of SNHG6 dramatically inhibited, whereas SNHG6 downregulation elevated, miR-543 expression (Fig. 4C). Moreover, miR-543 level in ovarian cancer tissues was lower than that in adjacent normal ovarian epithelial samples (0.495 [0.373, 0.593] vs 0.965 [0.815, 1.220], $P < 0.001$, Fig. 4D). And miR-543 level was negatively correlated with SNHG6 level in ovarian cancer tissues (Fig. 4E). Additionally, miR-543 mimic enhanced, but *anti*-miR-543 abrogated the effects of SNHG6 knockdown on the viability, migration, invasion and EMT-related gene expression in ovarian cancer cells (Fig. 4F–J; The original images of blots in Fig. 4J were attached in supplementary file 2). These results suggest that SNHG6 functions via binding to miR-543.

3.5. YAP1 is a target of miR-543

YAP1, a potent oncogene, was reported to be overexpressed in ovarian cancer [17]. We also found that YAP1 expression was increased in ovarian cancer tissues compared to the adjacent normal tissues (2.970 [1.900, 4.360] vs 0.960 [0.713, 1.270], $P < 0.001$, Fig. 5A). By using online software, we found YAP1 is a potential target of miR-543. The predicted binding site of YAP1 3′ untranslated
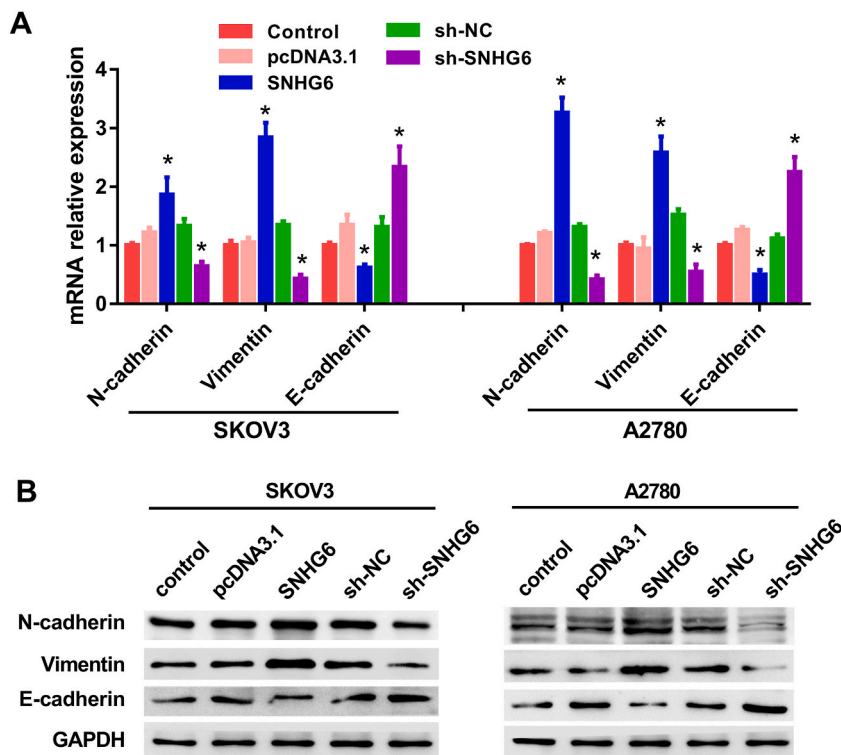
Fig. 3. SNHG6 contributes to the EMT of ovarian cancer cells. SKOV3 and A2780 cells were transfected with indicated vectors for 72 h. (A) The mRNA levels of N-cadherin, vimentin and E-cadherin were determined by qRT-PCR. (B) The protein levels of N-cadherin, vimentin and E-cadherin were analyzed by Western blot. *$P < 0.05$ vs the control group.

region (UTR) was shown in Fig. 5B. SKOV3 and A2780 cells were co-transfected with the wild-type or mutant YAP1 3′UTR vector and miR-543 mimic, and the results revealed that luciferase activity was notably decreased only in cells transfected with the wild-type vector (Fig. 5C and D). Additionally, we found that miR-543 mimic could suppress YAP1 expression both at transcription and translation levels (Fig. 5E and F; The original images of blots in Fig. 5F were attached in supplementary file 3). These data suggested that YAP1 is a target of miR-543.

3.6. SNHG6 interacts with miR-543 to enhance the malignant phenotypes of ovarian cancer cells via targeting YAP1

Online software showed that SNHG6 and YAP1 contained the same binding sequences of miR-543 (Figs. 4A and 5B). Hence, we hypothesized that SNHG6 might act via sponging miR-543 to regulate YAP1 expression in ovarian cancer cells. To verify this assumption, RIP analysis with anti-AGO2 antibody was performed in SKOV3 cells transfected with miR-543 mimic. SNHG6, YAP1 and miR-543 were together immunoprecipitated by anti-AGO2 after miR-543 overexpression (Fig. 6A). Furthermore, compared with the pcDNA3.1 control group, SNHG6 overexpression significantly elevated YAP1 expression. MiR-543 mimic reversed, but *anti*-miR-543 further enhanced, the effect of SNHG6 on YAP1 levels (Fig. 6B; The original images of blots in Fig. 6B were attached in supplementary file 4). In addition, the effects of YAP1 on ovarian cancer cells were verified by constructed pcDNA3.1-YAP1 plasmid, which markedly elevated YAP1 expression (Fig. 6C; The original images of blots in Fig. 6C were attached in supplementary file 5). The suppressed effects caused by SNHG6 silence on the viability, migration, invasion and EMT of ovarian cancer cells were all abolished by YAP1 upregulation (Fig. 6D–G; The original images of blots in Fig. 6C were attached in supplementary file 6).

4. Discussion

In the present study, SNHG6 was elevated both in ovarian cancer tissues and cells. High levels of SNHG6 were correlated with adverse clinicopathological features. Upregulation of SNHG6 significantly enhanced the malignant phenotypes of ovarian cancer cells. Silencing of SNHG6 showed the opposite effects. Moreover, we found that SNHG6 is a ceRNA for miR-543 to elevate YAP1 in ovarian cancer.

Previous studies assumed that small nucleolar RNAs (snoRNAs) only acted as cellular housekeeping RNA. Recently, it was found that snoRNAs could also control cell fate and oncogenesis [18,19]. SNHG6 had been reported to act as an oncogene in several cancers [4–7]. SNHG6 expression was significantly upregulated and was correlated with poor overall survival in a variety of tumors [9]. In this study, we demonstrated that SNHG6 levels were higher in ovarian cancer tissues than in adjacent normal ovarian epithelial samples.
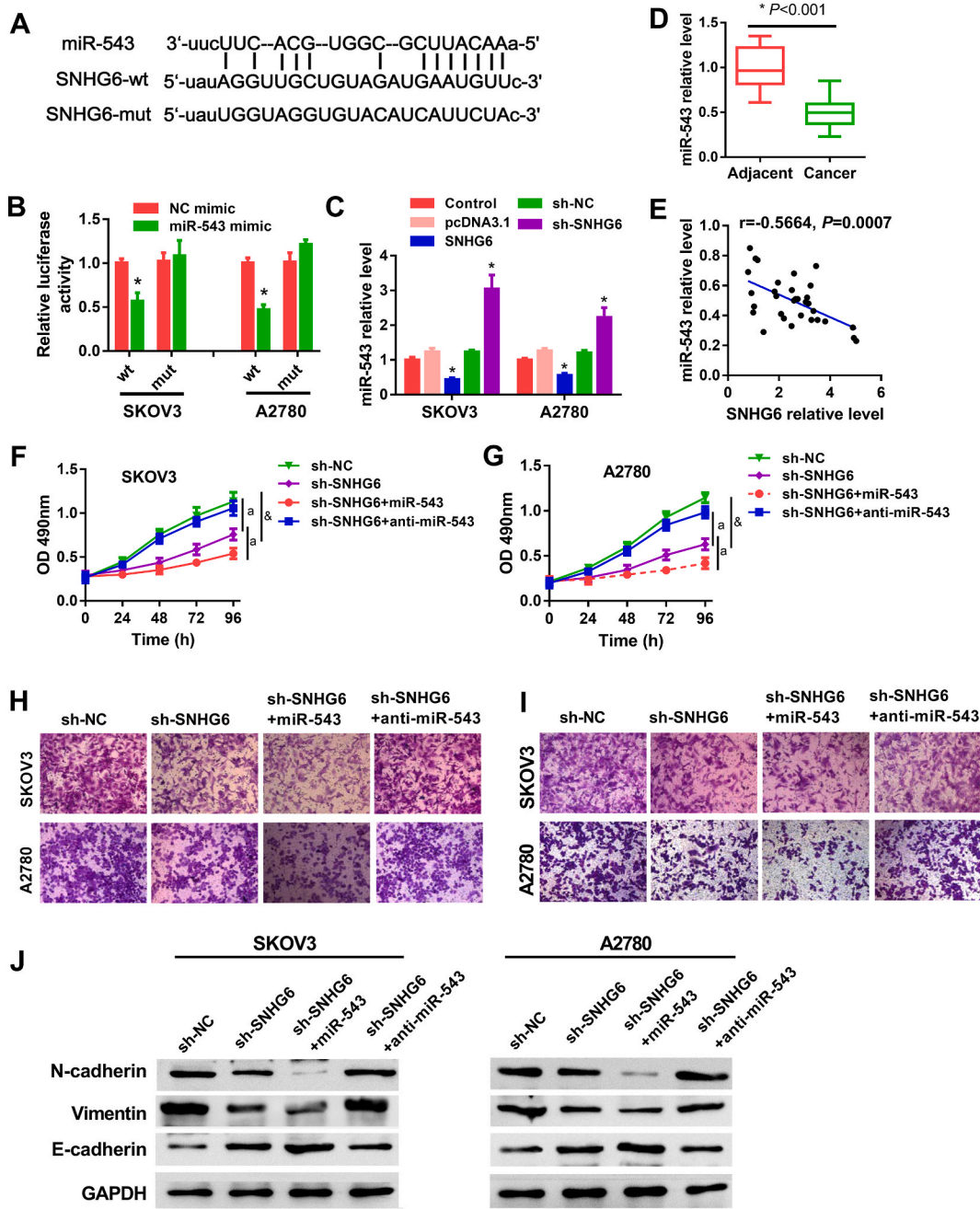
Fig. 4. SNHG6 functions through binding to and regulating miR-543 in ovarian cancer cells. (A) The binding sequences of miR-543 and SNHG6 as well as the mutant sequence of SNHG6. (B) Dual-fluorescence reporter gene assay confirmed that SNHG6 directly interacted with miR-543 in SKOV3 and A2780 cells. (C) miR-543 expression was analyzed by qRT-PCR after SNHG6 upregulation or downregulation. (D) The levels of miR-543 in 32 primary epithelial ovarian cancer tissues and adjacent normal ovarian epithelial samples. (E) The relationship between miR-543 and SNHG6 was analyzed in 32 primary epithelial ovarian cancer specimens. SKOV3 (F) and A2780 (G) cells were co-transfected with SNHG6 shRNA and miR-543 mimics or *anti*-miR-543, or transfected with SNHG6 shRNA or control shRNA (sh-NC) alone. Cell viability was measured by MTT. The migration (H) and invasion (I) of SKOV3 and A2780 cells were detected by transwell. (J) The protein levels of N-cadherin, vimentin and E-cadherin were analyzed by Western blot. *$P < 0.05$ vs the NC mimic group, #$P < 0.05$ vs the control group or the adjacent group, &$P < 0.05$ vs the sh-NC group, a$P < 0.05$ vs the sh-SNHG6 group.

Elevated SNHG6 levels were positively correlated with Grade, FIGO stage, and lymph node metastasis. In ovarian cancer cells, upregulation of SNHG6 promoted, whereas downregulation of SNHG6 suppressed the proliferation, migration, and invasion. These results suggested that SNHG6 acted as an oncogene in ovarian cancer, which was consistent with a previous study [10].
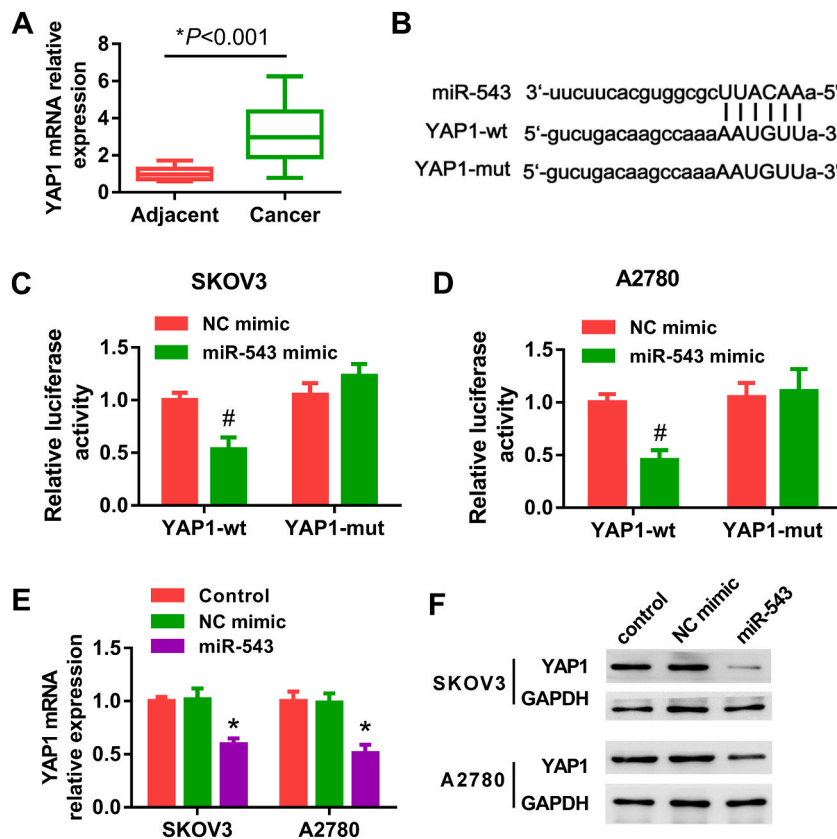
Fig. 5. YAP1 is a target of miR-543. (A) YAP1 mRNA expression in 32 primary epithelial ovarian cancer tissues and adjacent normal ovarian epithelial samples. (B) The potential binding site of miR-543 on YAP1. SKOV3 (C) and A2780 (D) cells were co-transfected with constructed YAP wild-type or mutant YAP1 luciferase reporter vector and miR-543 mimic or control mimic (NC mimic) for 48 h. The luciferase activity was determined. Ovarian cancer cells were transfected with miR-543 mimic or NC mimic for 48 h, and YAP1 mRNA (E) and protein (F) levels were detected by qRT-PCR or Western blot. *$P < 0.05$ vs the normal group or the control group, #$P < 0.05$ vs the NC mimic group.

The process of EMT is accompanied with the decrease of epithelial markers and increase of expression of mesenchymal genes. E-cadherin is the prototypical epithelial cell marker; N-cadherin and vimentin are important mesenchymal markers of EMT [20,21]. We demonstrated that upregulation of SNHG6 promoted the expression of N-cadherin and vimentin, but reduced E-cadherin level. And downregulation of SNHG6 elevated E-cadherin expression, but suppressed levels of N-cadherin and vimentin. Previous studies also reported that high levels of SNHG6 promoted EMT in other cancers, such as breast cancer [12], colorectal cancer [22], glioma [23] and gastric cancer [24]. The underlying molecular mechanisms by which SNHG6 promoted EMT were varied.

SNHG6 was reported to promote tumor progression by sponging miR-543 in breast cancer and glioma [12,13]. MiR-543 played vital roles in the progression of multiple cancers, such as breast cancer [25], liver cancer [26], and colorectal cancer [27]. MiR-543 performed different roles in different malignancies. MiR-543 acted as a tumor suppressor in ovarian cancer, and the expression of miR-543 was significantly decreased in ovarian cancer cell lines and ovarian cancer tissues [14,28]. Similar results were observed in the current study. The dual-fluorescence reporter gene assay confirmed the interaction between miR-543 and SNHG6. SNHG6 negatively regulated miR-543 in ovarian cancer cells. Additionally, the effects of SNHG6 silence on ovarian cancer were further strengthened by miR-543 mimic, but reversed by miR-543 inhibition. Taken together, these results demonstrated that SNHG6 functioned via binding to miR-543 and negatively regulating its expression in ovarian cancer cells. Besides, a previous study showed that SNHG6 promoted cell proliferation and migration through sponging miR-4465 to regulate EZH2 in ovarian clear cell carcinoma [10].

Several targets of miR-543 had been explored in ovarian cancers. MiR-543 could also suppress the proliferation and invasion in ovarian cancers by targeting TWIST1, MMP7 or SERPINI1 [15,28,29]. Upregulation of miR-543 led to increased ovarian cancer cells supernatant glucose levels and suppressed cell growth via targeting insulin-like growth factor 2 [14]. Here, we showed that YAP1 was a target of miR-543. YAP1 is a major effector of the Hippo signaling pathway. The Hippo pathway is often deregulated in human cancers, leading to the loss of control on YAP1 expression. Enhanced YAP1 expression induces EMT and augments drug resistance in cancers [30]. It is a direct oncogenic target in various tumor types including ovarian cancer [17,31]. Studies showed that YAP1 expression was increased and regulated the progression of ovarian cancer [32,33]. We also showed the YAP1 level was higher in ovarian cancer tissues than that in adjacent normal tissues. Considering SNHG6 mainly acted as a ceRNA in many cancers [4,7,8], we speculated that SNHG6 acts as a ceRNA for miR-543. RIP analysis with anti-AGO2 confirmed that SNHG6 and YAP1 both directly bound to miR-543.
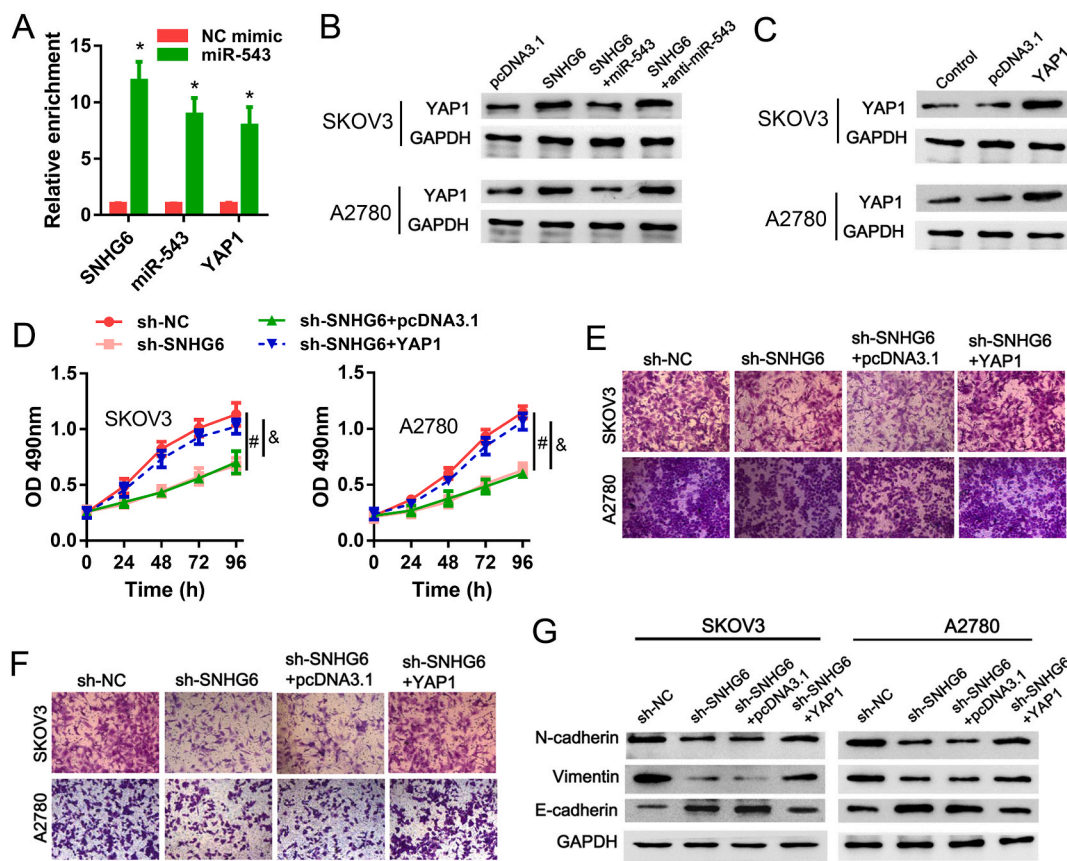
Fig. 6. SNHG6 as a ceRNA for miR-543 to regulate YAP1 expression to promote the malignant phenotypes of ovarian cancer cells. (A) SKOV3 cells were transfected with miR-543 mimic or NC mimic. The levels of SNHG6, YAP1 and miR-543 were analyzed in cell lysates immunoprecipitated using anti-AGO2 antibody. (B) YAP1 protein expression was analyzed in SKOV3 and A2780 cells transfected with pcDNA3.1-SNHG6 with or without miR-543 mimic/*anti*-miR-543. (C) Ovarian cancer cells were transfected with constructed pcDNA3.1-YAP1 plasmid, and YAP1 expression was determined by Western blot. (D) SKOV3 and A2780 cells were co-transfected with SNHG6 shRNA and pcDNA3.1-YAP1 plasmid or its control pcDNA3.1. Cell viability was analyzed by MTT. (E) and (F) Transwell assay for the migration and invasion of SKOV3 and A2780 cells. (G) The protein levels of N-cadherin, vimentin, and E-cadherin were analyzed by Western blot. $^*P < 0.05$ vs the NC mimic group, $^#P < 0.05$ vs the sh-NC group, $^&P < 0.05$ vs the sh-SNHG6 group.

Moreover, overexpression of SNHG6 notably increased YAP1 expression. This effect was reversed by miR-543 mimic, but was enhanced by miR-543 inhibitors. Additionally, YAP1 overexpression significantly abrogated, at least partially, the effects of SNHG6 downregulation on the viability, migration, invasion and EMT of ovarian cancer. These data suggested that SNHG6 promoted the malignant phenotypes via sponging miR-543 to enhance YAP1 expression in ovarian cancer cells.

SNHG6 level was positively correlated with Grade, FIGO stage and lymph node metastasis of ovarian cancer patients. However, Wu [10] showed that SNHG6 level was not correlated with FIGO stage and lymph node metastasis, but was strongly associated with vascular invasion and distant metastasis. This inconsistent conclusion may be due to the differences between samples and the small sample size. Although the test power indicated that the sample size of this study was sufficient and the results were credible, the small sample size is a limitation of this study. The relationship between SNHG6, miR-543 and clinicopathological characteristics should be investigated in a larger sample size. Due to the numerous targets of SNHG6, and numerous targets of its downstream micoRNA, SNHG6 might regulate tumor progression in a very complex regulatory network. In the current study, we only focused on the miR-543/YAP1 pathway. This is another limitation of this study.

5. Conclusions

The present study demonstrates that SNHG6 performed its oncogenic role via miR-543/YAP1 pathway in ovarian cancer. This finding improves our understanding of SHNG6 acts as a competing endogenous RNA for miR-543 to elevate YAP1 expression. The current study indicates SNHG6 and miR-543 are potential candidates for a crucial therapeutic and diagnostic biomarker for ovarian cancer. Further study with a lager sample size is needed to verify the correlation of SNHG6, miR-543 and YAP1 with clinicopathological characteristics in patients with ovarian cancer. The *in vivo* study is also necessary to clarify the mechanism of the oncogenic function of SNHG6.

Author contribution statement

Mengya Su: Conceived and designed the experiments; Performed the experiments; Analyzed and interpreted the data; Wrote the paper. Ping Huang: Performed the experiments; Contributed reagents, materials, analysis tools or data; Wrote the paper. Qian Li: Performed the experiments; Wrote the paper.

Data availability statement

Data will be made available on request.

Declaration of competing interest

The authors declare that they have no known competing financial interests or personal relationships that could have appeared to influence the work reported in this paper.

Appendix A. Supplementary data

Supplementary data related to this article can be found at https://doi.org/10.1016/j.heliyon.2023.e16291.

References

[1] S. Lheureux, C. Gourley, I. Vergote, A.M. Oza, Epithelial ovarian cancer, Lancet 393 (2019) 1240–1253.

[2] L.A. Torre, B. Trabert, C.E. DeSantis, K.D. Miller, G. Samimi, C.D. Runowicz, M.M. Gaudet, A. Jemal, R.L. Siegel, Ovarian cancer statistics, CA A Cancer J. Clin. 68 (2018) 284–296.

[3] M. Buechel, T.J. Herzog, S.N. Westin, R.L. Coleman, B.J. Monk, K.N. Moore, Treatment of patients with recurrent epithelial ovarian cancer for whom platinum is still an option, Ann. Oncol. 30 (2019) 721–732.

[4] C. Cao, T. Zhang, D. Zhang, L. Xie, X. Zou, L. Lei, D. Wu, L. Liu, The long non-coding RNA, SNHG6-003, functions as a competing endogenous RNA to promote the progression of hepatocellular carcinoma, Oncogene 36 (2017) 1112–1122.

[5] Y. Li, D. Li, M. Zhao, S. Huang, Q. Zhang, H. Lin, W. Wang, K. Li, Z. Li, W. Huang, Y. Che, C. Huang, Long noncoding RNA SNHG6 regulates p21 expression via activation of the JNK pathway and regulation of EZH2 in gastric cancer cells, Life Sci. 208 (2018) 295–304.

[6] M. Li, Z. Bian, S. Yao, J. Zhang, G. Jin, X. Wang, Y. Yin, Z. Huang, Up-regulated expression of SNHG6 predicts poor prognosis in colorectal cancer, Pathol. Res. Pract. 214 (2018) 784–789.

[7] C. Wang, W. Tao, S. Ni, Q. Chen, Upregulation of lncRNA snoRNA host gene 6 regulates NUAK family SnF1-like kinase-1 expression by competitively binding microRNA-125b and interacting with Snail1/2 in bladder cancer, J. Cell. Biochem. 120 (2019) 357–367.

[8] P. Lv, X. Qiu, Y. Gu, X. Yang, X. Xu, Y. Yang, Long non-coding RNA SNHG6 enhances cell proliferation, migration and invasion by regulating miR-26a-5p/MAPK6 in breast cancer, Biomed. Pharmacother. 110 (2019) 294–301.

[9] S. Zhao, H. Zhu, R. Jiao, X. Wu, G. Ji, X. Zhang, Prognostic and clinicopathological significance of SNHG6 in human cancers: a meta-analysis, BMC Cancer 20 (2020) 77.

[10] Y. Wu, Y. Deng, Q. Guo, J. Zhu, L. Cao, X. Guo, F. Xu, W. Weng, X. Ju, X. Wu, Long non-coding RNA SNHG6 promotes cell proliferation and migration through sponging miR-4465 in ovarian clear cell carcinoma, J. Cell Mol. Med. 23 (2019) 5025–5036.

[11] M. Cesana, D. Cacchiarelli, I. Legnini, T. Santini, O. Sthandier, M. Chinappi, A. Tramontano, I. Bozzoni, A long noncoding RNA controls muscle differentiation by functioning as a competing endogenous RNA, Cell 147 (2011) 358–369.

[12] Y.Q. Wang, G. Huang, J. Chen, H. Cao, W.T. Xu, LncRNA SNHG6 promotes breast cancer progression and epithelial-mesenchymal transition via miR-543/LAMC1 axis, Breast Cancer Res. Treat. 188 (2021) 1–14.

[13] Y. Zhang, J. An, Y. Pei, LncRNA SNHG6 promotes LMO3 expression by sponging miR-543 in glioma, Mol. Cell. Biochem. 472 (2020) 9–17.

[14] S. Zhang, D. Pan, Q. Wu, L. Zhen, S. Liu, J. Chen, R. Lin, Q. Hong, X. Zheng, H. Yi, Exosomal miR-543 inhibits the proliferation of ovarian cancer by targeting IGF2, J. Immunol. Res. 2022 (2022), 2003739.

[15] Q. Yu, Z. Zhang, B. He, H. Wang, P. Shi, Y. Li, MiR-543 functions as tumor suppressor in ovarian cancer by targeting TWIST1, J. Biol. Regul. Homeost. Agents 34 (2020) 101–110.

[16] X. Zhou, W. Zhang, M. Jin, J. Chen, W. Xu, X. Kong, lncRNA MIAT functions as a competing endogenous RNA to upregulate DAPK2 by sponging miR-22-3p in diabetic cardiomyopathy, Cell Death Dis. 8 (2017) e2929.

[17] H. Yan, H. Li, P. Li, X. Li, J. Lin, L. Zhu, M.A. Silva, X. Wang, P. Wang, Z. Zhang, Long noncoding RNA MLK7-AS1 promotes ovarian cancer cells progression by modulating miR-375/YAP1 axis, J. Exp. Clin. Cancer Res. 37 (2018) 237.

[18] E.S. Martens-Uzunova, S.E. Jalava, N.F. Dits, G.J. van Leenders, S. Moller, J. Trapman, C.H. Bangma, T. Litman, T. Visakorpi, G. Jenster, Diagnostic and prognostic signatures from the small non-coding RNA transcriptome in prostate cancer, Oncogene 31 (2012) 978–991.

[19] H.E. Gee, F.M. Buffa, C. Camps, A. Ramachandran, R. Leek, M. Taylor, M. Patil, H. Sheldon, G. Betts, J. Homer, C. West, J. Ragoussis, A.L. Harris, The small-nucleolar RNAs commonly used for microRNA normalisation correlate with tumour pathology and prognosis, Br. J. Cancer 104 (2011) 1168–1177.

[20] M. Zeisberg, E.G. Neilson, Biomarkers for epithelial-mesenchymal transitions, J. Clin. Invest. 119 (2009) 1429–1437.

[21] S.J. Serrano-Gomez, M. Maziveyi, S.K. Alahari, Regulation of epithelial-mesenchymal transition through epigenetic and post-translational modifications, Mol. Cancer 15 (2016) 18.

[22] X. Wang, Q. Lai, J. He, Q. Li, J. Ding, Z. Lan, C. Gu, Q. Yan, Y. Fang, X. Zhao, S. Liu, LncRNA SNHG6 promotes proliferation, invasion and migration in colorectal cancer cells by activating TGF-beta/Smad signaling pathway via targeting UPF1 and inducing EMT via regulation of ZEB1, Int. J. Med. Sci. 16 (2019) 51–59.

[23] J. Nie, Y. Feng, H. Wang, X.Y. Lian, Y.F. Li, Long non-coding RNA SNHG6 supports glioma progression through upregulation of Notch1, Sox2, and EMT, Front. Cell Dev. Biol. 9 (2021), 707906.

[24] K. Yan, J. Tian, W. Shi, H. Xia, Y. Zhu, LncRNA SNHG6 is associated with poor prognosis of gastric cancer and promotes cell proliferation and EMT through epigenetically silencing p27 and sponging miR-101-3p, Cell. Physiol. Biochem. 42 (2017) 999–1012.

[25] P. Chen, W. Xu, Y. Luo, Y. Zhang, Y. He, S. Yang, Z. Yuan, MicroRNA 543 suppresses breast cancer cell proliferation, blocks cell cycle and induces cell apoptosis via direct targeting of ERK/MAPK, OncoTargets Ther. 10 (2017) 1423–1431.

[26] L. Yu, L. Zhou, Y. Cheng, L. Sun, J. Fan, J. Liang, M. Guo, N. Liu, L. Zhu, MicroRNA-543 acts as an oncogene by targeting PAQR3 in hepatocellular carcinoma, Am J Cancer Res 4 (2014) 897–906.

[27] C. Fan, Y. Lin, Y. Mao, Z. Huang, A.Y. Liu, H. Ma, D. Yu, A. Maitikabili, H. Xiao, C. Zhang, F. Liu, Q. Luo, G. Ouyang, MicroRNA-543 suppresses colorectal cancer growth and metastasis by targeting KRAS, MTA1 and HMGA2, Oncotarget 7 (2016) 21825–21839.

[28] N. Song, H. Liu, X. Ma, S. Zhang, Placental growth factor promotes metastases of ovarian cancer through MiR-543-regulated MMP7, Cell. Physiol. Biochem. 37 (2015) 1104–1112.

[29] C. Qu, C. Dai, Y. Guo, R. Qin, J. Liu, Long non-coding RNA PVT1-mediated miR-543/SERPINI1 axis plays a key role in the regulatory mechanism of ovarian cancer, Biosci. Rep. 40 (2020).

[30] S. Nagashima, Y. Bao, Y. Hata, The Hippo pathway as drug targets in cancer therapy and regenerative medicine, Curr. Drug Targets 18 (2017) 447–454.

[31] H. Yagi, K. Asanoma, T. Ohgami, A. Ichinoe, K. Sonoda, K. Kato, GEP oncogene promotes cell proliferation through YAP activation in ovarian cancer, Oncogene 35 (2016) 4471–4480.

[32] C. He, X. Lv, G. Hua, S.M. Lele, S. Remmenga, J. Dong, J.S. Davis, C. Wang, YAP forms autocrine loops with the ERBB pathway to regulate ovarian cancer initiation and progression, Oncogene 34 (2015) 6040–6054.

[33] Y. Xia, T. Chang, Y. Wang, Y. Liu, W. Li, M. Li, H.Y. Fan, YAP promotes ovarian cancer cell tumorigenesis and is indicative of a poor prognosis for ovarian cancer patients, PLoS One 9 (2014), e91770.